 doi:10.20944/preprints202202.0126.v1

Article

Roach Infestation Optimization MPPT Algorithm for Solar Photovoltaic System

Chittaranjan Pradhan[1,*], Nicholas Kakra Ntiakoh[1] and Rajnish Kaur Calay[2]

[1] Arctic Centre for Sustainable Energy, Department of Electrical Engineering, The University of Tromsø -UiT Arctic University of Norway, Narvik Campus, Norway-8514; chittaranjan.pradhan@uit.no; nicholaskakra@gmail.com
[2] Department of Building, Energy and Material Technology, UiT The Arctic University of Norway, Narvik Campus, Norway-8514; rajnish.k.calay@uit.no
* Correspondence: chittaranjan.pradhan@uit.no

Abstract: Of all the renewable energy sources, solar photovoltaic (PV) power is estimated to be a popular source due to several advantages such as its free availability, absence of rotating parts, integration to building such as rooftops and less maintenance cost. The nonlinear current–voltage (I–V) characteristics and power generated from a PV array primarily depend on solar insolation/irradiation and panel temperature. The extracted PV output power is influenced by the accuracy with which the nonlinear power–voltage (*P–V*) characteristic curve is traced by the maximum power point tracking (MPPT) controller. In this paper, a bio-inspired roach infestation optimization (RIO) algorithm is proposed to extract the maximum power from the PV system (PVS). To validate the usefulness of the RIO MPPT algorithm, MATLAB/Simulink simulations are performed under varying environmental conditions, for example, step changes in solar irradiance, and partial shading of the PV array. Furthermore, the search performance of the RIO algorithm is examined on different unconstrained benchmark functions, and it is that realized that the RIO algorithm has improved convergence characteristics in terms of finding the optimal solution than Particle swarm optimization (PSO). The results demonstrated that the RIO-based MPPT performs remarkably in tracking with high accuracy as the PSO-based MPPT.

Keywords: DC-DC Boost converter; Maximum power point tracking (MPPT); Partial shading condition (PSC); Particle swam optimization (PSO); Roach infestation optimization (RIO); Solar photovoltaic system.

1. Introduction

The use of non-renewable energy sources such as oil, coal, and natural gas for the production of electricity produces harmful emissions that affect the environment and cause global warming. The urgent necessity to protect this planet has called for cleaner sources of energy, of which solar power plays a significant role. Solar is a pollution-free source of energy, and it is abundantly available. The global growth of solar PV capacity has been increased consistently since 2000. Between 2000 and 2019, numbers grew by 632.4 gigawatts. In 2019, solar PV capacity reached 633.7 gigawatts globally, with 116.9 gigawatts installed that year [1]. **Figure 1** illustrates the aggregated solar PV capacity in gigawatts by select countries as of 2019.

Photovoltaics (PVs) is converting light (from the sun) into electricity by the use of semiconductor materials that shows the photovoltaic effect. A PV system utilizes solar modules, which comprise several solar cells, generating electrical energy or power [2-4]. Despite the recent technological enhancement in PV operational characteristics, such as reducing costs and improving efficiency, the lower energy conversion efficiency of PV systems (PVSs) remains a significant drawback to the utilization of PV power. One other major issue with PV power generation is the reliance on environmental influences, such

Preprints (www.preprints.org) | NOT PEER-REVIEWED | Posted: 9 February 2022 doi:10.20944/preprints202202.0126.v1

as solar irradiance and ambient temperature [5-7]. Since the cost involved in PV power generation is high and to make more profit on investment, it is very essential to extract most of the available solar energy through the panels. Therefore, the control unit of the PV system must be compelled through an efficient MPPT method for harvesting the maximum power from the installed PV arrays by generating an appropriate duty ratio to regulate the DC-DC converter embedded in the system [8-10]. In [9], a comprehensive review of the DC–DC converter topologies and their modulation strategies for solar PV systems. Taking into account all affecting factors of the PV, boosting the MPPT efficacy using a low-cost hardware approach is essential to improving the operation of the PVS [11-13].

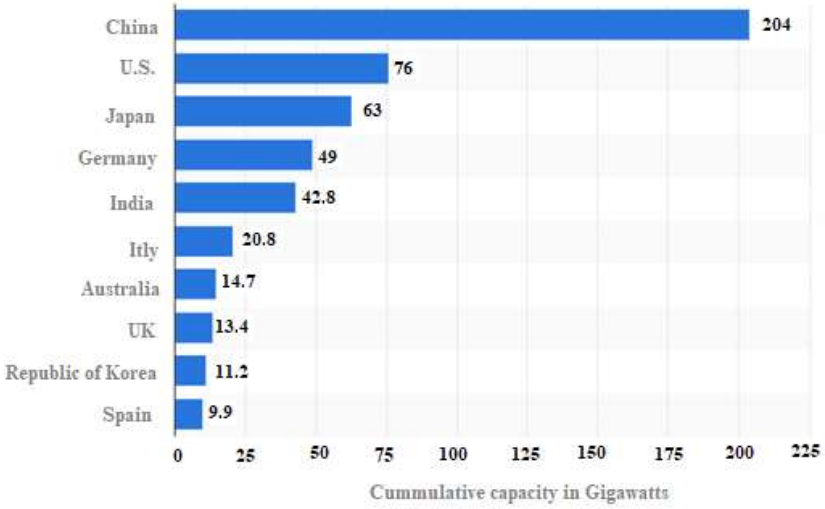

Figure 1. Global cumulative solar PV capacity in 2019 [1]

The objective of an efficient MPPT controller is to meet the ensuing characteristics such as accuracy, robustness, and faster-tracking speed under partial shading conditions (PSCs) and climatic variations such as a change in solar irradiation and temperature. To realize these objectives, numerous traditional techniques in artificial intelligence and bio-inspired approaches/algorithms have been recommended in the previous literature [13-16]. The most common conventional MPPT methods are the incremental conductance (IC) [17], perturb and observe (P&O) [18], and hill-climbing (HC) [19]. These conventional methods are simple, easy implementation, and can track the MPP effectively under normal environmental circumstances. However, they have a disadvantage as continuous oscillations follow around the MPP, causing significant power loss in the steady-state condition. In this perspective, various artificial intelligent MPPT methodologies have been implemented to handle the shortcomings of the conventional MPPT methods, especially highly intermittent conditions. These include fuzzy logic control (FLC) [20], artificial neural network (ANN) [21], firefly algorithm (FA) [22], PSO [23], ant colony optimization (ACO) [24], flower pollination algorithm (FPA) [25], invasive weed optimization [26], salp swarm optimization [27], bat optimization [28], Neighboring-Pixel-based virtual imaging technique [29], surface-based polynomial fitting [30], Jaya algorithm [31], most valuable player algorithm [32] and many more. The results demonstrated that the artificial intelligence algorithms have high accuracy and stability in tracking the global MPP in different environmental conditions.

In practice, each intelligent technique can only be employed in its best performance in a desirable scenario and is generally not fitting for a wide range of applications [16, 33]. From this perspective, applying or designing a new intelligent algorithm has been always welcome, for improving the search performance [33-34]. By Seeing the efficacy of the soft-computing based intelligent optimization algorithms, in this paper, a bio-inspired Roach

Preprints (www.preprints.org) | NOT PEER-REVIEWED | Posted: 9 February 2022 doi:10.20944/preprints202202.0126.v1

Infestation Optimization (RIO) for obtaining the maximum power from the PV is projected.

The main contributions of this work can be summarized as follows:

- The paper presents the RIO algorithm to track the GMPP of the PV system.
- The efficacy of the proposed RIO algorithm has a tested in different unconstrained benchmark functions and as well as MPPT of the PV system for both symmetrical irradiation and PSCs.
- The proposed population-based RIO technique achieves excellence-searching performance in terms of convergence time and accuracy as compared to PSO.

The paper is organized as follows. Section 2 addresses the studied PV system. In Section 3, an overview of the RIO algorithm is explained. The Simulation results and discussions are provided in Section 4. Finally, the conclusion and future work is illustrated in Section 5.

2. Studied Photovoltaic (PV) System

To establish the behavior of a solar cell electronically, an equivalent model is made based on basic electrical components. The solar cell is modeled by a current source in parallel with a diode, a shunt resistance and a series resistance component as presented in **Figure 2** [7]. The detailed mathematical modeling of the PV cell is taken from [26].

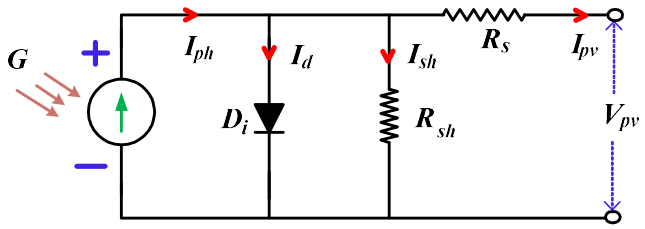

Figure 2. Equivalent model of a solar cell

In **Figure 2**, R_s and R_{sh} are the intrinsic series and shunt resistor of the PV cell (Ω), respectively. I_{sh} is the current through R_{sh}. D_i is the intrinsic diode. I_d is diode current (A), I_{sh} is shunt current (A), I_{ph} is the light-generated current in the cell (A). V_{pv} and I_{pv} are the PV output voltage (V) and current (A), respectively. G is the solar irradiation (W/m²).

In **Figure 2**, the current generated by the solar cell is equivalent to that produced by the current source minus that which flows through the diode and the shunt resistor which is established by Kirchhoff's current law as follows [19]:

$$I_{pv} = I_{ph} - I_d - I_{sh} \tag{1}$$

The current through these elements can be given by the voltages across them:

$$V_d = V_{pv} + R_s I_{pv} \tag{2}$$

Where, V_d is the voltage across the diode (V).

The PV cell is quantified by current-voltage characteristic operation as follows [19]:

Preprints (www.preprints.org) | NOT PEER-REVIEWED | Posted: 9 February 2022 doi:10.20944/preprints202202.0126.v1

$$I_{pv} = n_p I_{ph} - n_p I_p \left[\exp\left(\frac{q(V_{pv} + I_{pv} R_s)}{A K T n_s} \right) - 1 \right] - \left(\frac{V_{pv} + I_{pv} R_s}{R_{sh}} \right) \quad (3)$$

with $$I_p = I_{rs} \left[\frac{T}{T_r} \right]^3 \exp\left(\frac{q V_{oc}}{AK} \left[\frac{1}{T_r} - \frac{1}{T} \right] \right), \quad I_{ph} = I_{sc} + [K(T_0 - T_r)] \frac{G}{1000}$$

where, n_s and n_p are the number of cells connected in series and parallel, q is the electron charge (C), K is Boltzmann's constant (J/K), A is the p-n junction's idealistic factor, T is the cell's absolute temperature (^{0}K), T_r is the cell reference temperature (^{0}K), I_{ph} is the cell's photocurrent (it depends on the solar irradiance and temperature), I_{rs} is the cell's reverse saturation current, I_{sc} is the short-circuit current of the PV cell, V_{oc} is the open-circuit voltage of the PV cell *and* G is the solar irradiance.

The studied PV system (PVS) consists of four-series (4S) connected PV modules, a resistive load, and a non-isolated DC-DC boost converter with the MPPT technique. The DC-DC converter acts as an interface between the PV panel and the load, allowing the follow-up of the maximum power. The MATLAB/Simulink model of the studied PVS is shown in **Figure 3**. The modeling parameters of the PVS and DC-DC converter are given in **Tables 1** and **2**, respectively. The detailed modeling and selection of the DC-DC boost converter components/parameters are taken from [36-37].

Table 1. Studied PV system parameters

System parameters/data	Symbol	Value
For one PV module		
Maximum power for 1000W/m² and 25^{0}C	P_{pv}^{max}	59.85W
Voltage at MPP for 1000W/m² and 25^{0}C	V_{pv}^{max}	17.1V
Current at MPP for 1000W/m² and 25^{0}C	I_{pv}^{max}	3.5A
Open-circuit voltage	V_{oc}	21.1V
Short-circuit current	I_{sc}	3.8A
Series resistance	R_s	0.10363 Ω
Shunt resistance	R_{sh}	283.3724 Ω
Ideality factor	A_0	1.5406
Temperature co-efficient of *Isc*		0.00247 %/°C
Temperature co-efficient of V_{oc}		-0.8 %/°C

Table 2. DC-DC boost converter parameters

System parameters/data	Symbol	Value
Capacitor	C	464μF
Input filter capacitor	C_i	10μF
Inductor	L	1.14mH
Switching frequency	f_s	50kHz
Load resistance	R	53 Ω

Preprints (www.preprints.org) | NOT PEER-REVIEWED | Posted: 9 February 2022 doi:10.20944/preprints202202.0126.v1

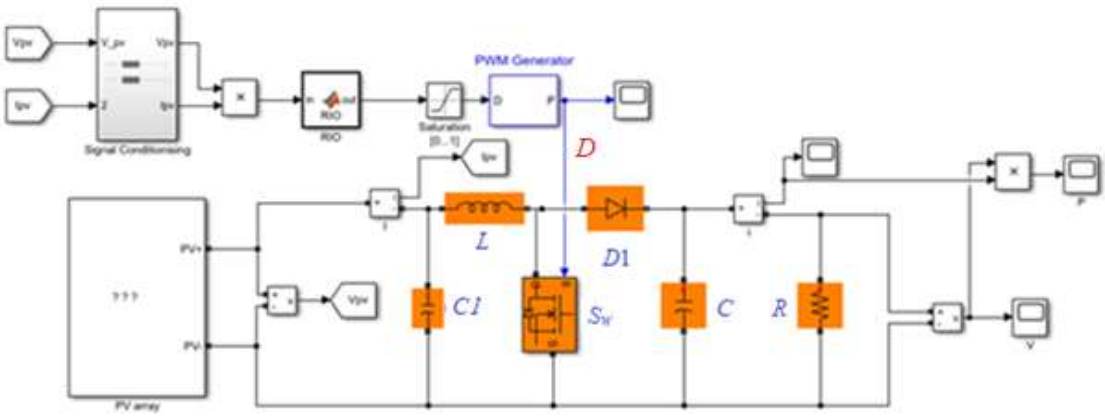

Figure 3. Simulink diagram of the studied PV system

In **Figure 3**, *R* is the load resistance. *L* and *C* are the boost converter inductor and capacitor, respectively. S_w is the power electronics switch (e.g., MOSFET). D_1 is the free-wheeling diode, C_1 is the input filter capacitor and *D* is the duty ratio.

3. Roach Infestation Optimization (RIO) Based MPPT Algorithm

The RIO was originally introduced by Haven *et al.*, as a cockroach-inspired algorithm [38]. The RIO was adapted from the traditional PSO algorithm, and therefore it has some parameters similar to the PSO. It is studied that cockroaches dislike the light and like the gathering [38]. Whenever a cockroach encounters another neighboring cockroach, it stops and socializes. During this period, information about the darkest known location is shared. When a cockroach is hungry it leaves friends and comfortable shelter and searches for food. The equation that models to find the Darkness behavior of a cockroach is evaluated as follows [38]:

$$v_i^{l+1} = C_0 v_i^{l} + C_{\max} R_1 * (p_i^{best} - x_i^{l}) \tag{4}$$

where, v^{l}_i represents the velocity of i^{th} particle/agent (i.e., cockroach) for the l^{th} iteration, x^{l}_i is the current location for the l^{th} iteration, p_i^{best} is the best dark place (location) of the i^{th} agent, C_o and C_{max} are constants and R_1 is a random number.

If a cockroach comes within a detection radius of another cockroach, they stop, and these cockroaches will group and share information by adapting the darkest local place L_i^{best} in the search space.

$$L_i^{best} = \arg\min\{\text{Function}(p_k)\}, k = \{i, j\} \tag{5}$$

where, (*i*, *j*) are the represents of the two socializing cockroaches and p_k is the darkest recognized place for the individual cockroach. Now, (4) can be presented as follows:

$$v_i^{l+1} = c_0 v_i^{l} + c_{\max} r_i * (P_i^{best} - x_i^{l}) + c_{\max} r_2 * (L_i^{best} - x_i^{l}) \tag{6}$$

Preprints (www.preprints.org) | NOT PEER-REVIEWED | Posted: 9 February 2022 doi:10.20944/preprints202202.0126.v1

It is noticeable that (6) is very much similar to the PSO velocity update. While the global best is substituted by a group best L_i^{best} in RIO.

Table 3. Parameters for RIO [38] and PSO [39] algorithms

Optimization algorithm	parameter	Symbols	value
RIO*	Cockroach parameter	C_0	0.4
	Cockroach parameter	C_{max}	1.4
PSO	Cognitive parameter	c_1	1.2
	Social parameter	c_2	1.6
	Weight parameter	w	0.4

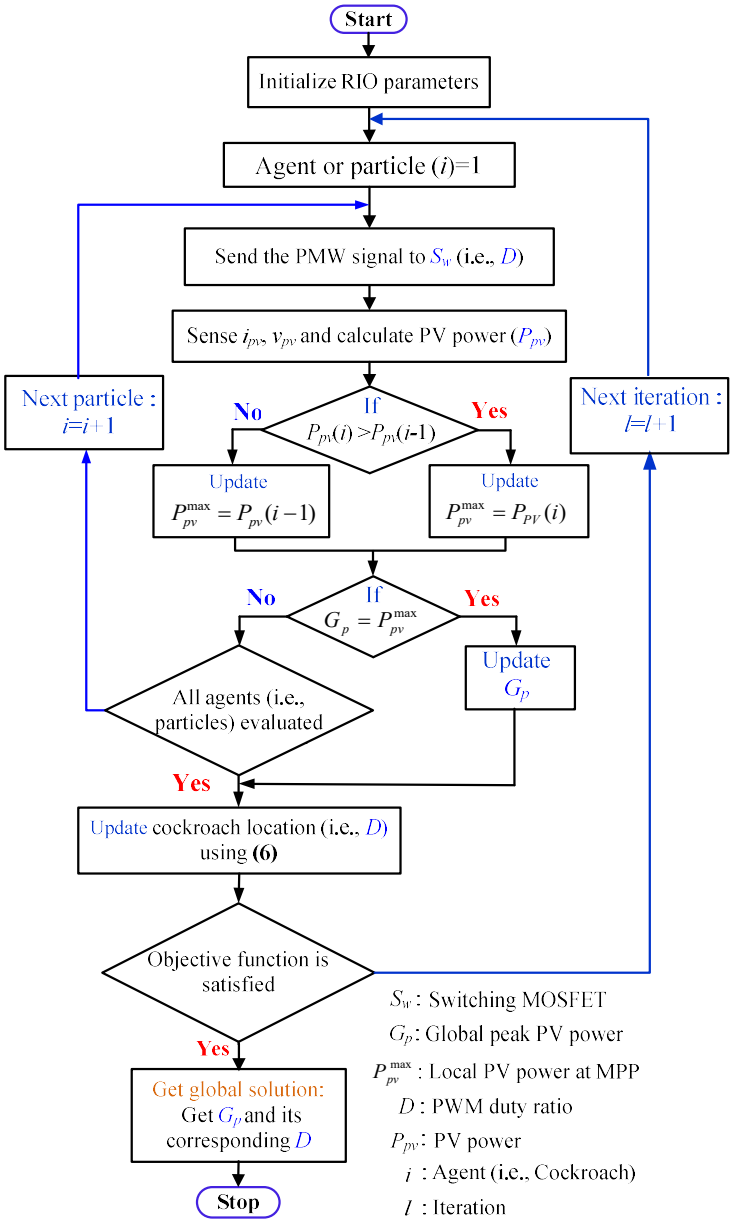

Figure 4. Flowchart of proposed RIO algorithm for MPPT

Preprints (www.preprints.org) | NOT PEER-REVIEWED | Posted: 9 February 2022 doi:10.20944/preprints202202.0126.v1

The flowchart of the RIO for MPPT is presented in **Figure 4.** To obtain the results, the value of the algorithm-specified control parameters of the PSO and RIO algorithms is given in **Table 3**. The DC-DC boost converter receives the PV voltage (V_{pv}) and current (I_{pv}) from the PVS and subsequently regulates it by adjusting the duty ratio (D). The value of D is updated using the optimization algorithms to achieve the MPP as shown in **Figure 3**. In this work, the global peak power (G_P) of the PV system is attained using the optimization algorithm to update D in the search process during both uniform irradiation/temperature and PSCs**.**

4. Results and Discussions

A MATLAB/Simulink (R2020b) software is employed for modeling and to justify the effectiveness of the RIO-based MPPT method of the PV system (**Figure 3**). Different case studies have been realized to show the efficacy of the RIO algorithm than PSO for getting the optimal solution of different unconstrained benchmark functions and GMPP of the PV system. The time-domain simulations have been accomplished for both uniform irradiation and PSCs such as (i). Uniform solar irradiance (Patterns-1, 2 and 5) and (ii). PSCs (Patterns-3, 4 and 6) as shown in **Figure 5**. **Table 4** illustrates the combination of various patterns selected for the PVS to plot the graphs. In the case of uniform/symmetrical solar irradiance, both solar irradiance and temperature remain constant, whereas, for PSCs, different values of solar irradiation (G) are considered, for the PV modules. The PVS is simulated under the various scenarios and the simulation results are demonstrated which are discussed below:

Table 4. Shading patterns of PVS for different solar irradiation (G)

Shading pattern		Module-1	Module-2	Module-3	Module-4
Pattern-1 at 25^{0}C	Symmetrical shading	10000	1000	1000	1000
Pattern-2 at 25^{0}C	Symmetrical shading	600	600	600	600
Pattern-3 at 25^{0}C	Partial shading	1000	800	600	400
Pattern-4 at 25^{0}C	Partial shading	800	600	400	200
Pattern-5 at 20^{0}C	Symmetrical shading	1000	1000	1000	1000
Pattern-6 at 20^{0}C	Partial shading	800	600	400	200

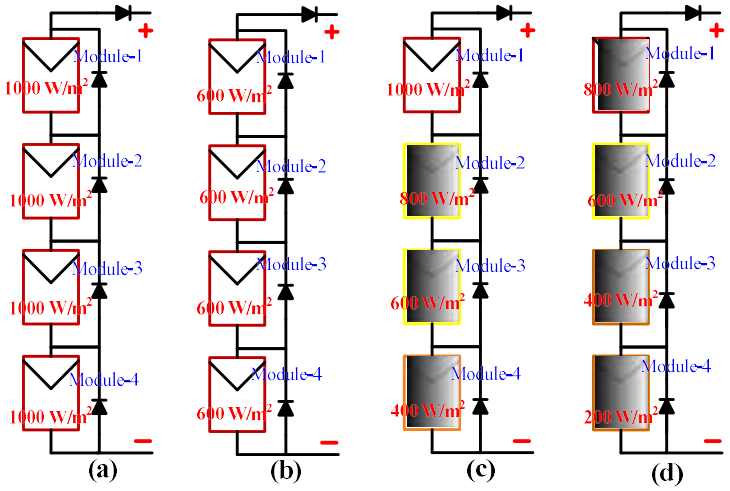

Figure 5. 4S structure of PV array system **(a).** Pattern-1, **(b).** Pattern-2, **(c).** Pattern-3, **(d).** Pattern-4

Preprints (www.preprints.org) | NOT PEER-REVIEWED | Posted: 9 February 2022 doi:10.20944/preprints202202.0126.v1

3.1. P-V and I-V characteristics curves of the PV system

The performance of a solar panel affects both uniform irradiation/temperature and PSCs. The PV system, whether a module, string, or array exhibits a *P-V* curve exhibiting multiple peaks, a Global Maximum Power Point (GMPP) which is the highest peak and Local Maximum PowerPoints (LMPPs) are the other multiple peaks. The *P-V* and *I-V* graphs under each pattern are given in **Figures 6** and **7**, respectively. From the figures, it can be noticed that the higher the solar irradiation, the peak PV will be higher and vice-versa. The same can be observed for other combinations of solar irradiation and temperature. The exact value of the global peak power (G_p), the corresponding voltage (V_{mpp}), and current (I_{mpp}) at MPP of the PVS under the selected test patterns are given in **Table 5**.

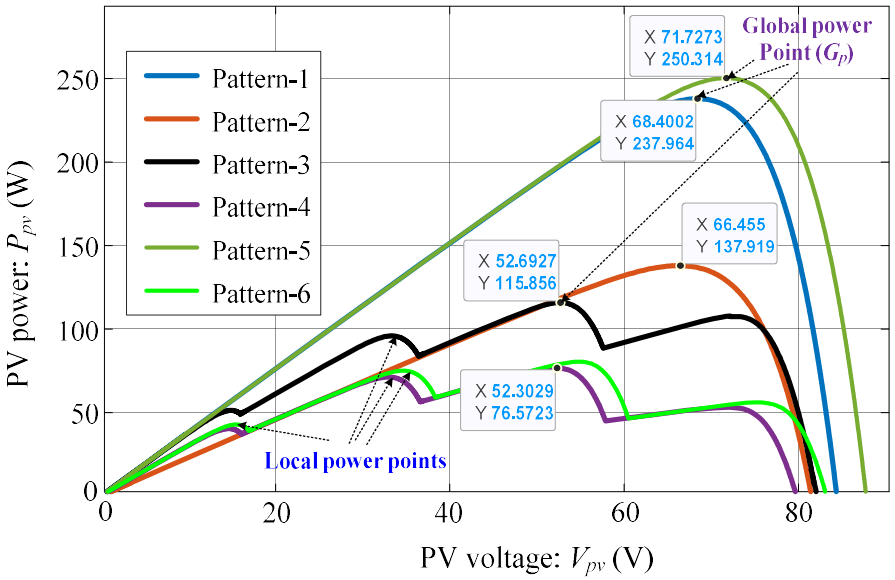

Figure 6. *P-V* graph for different shading patterns

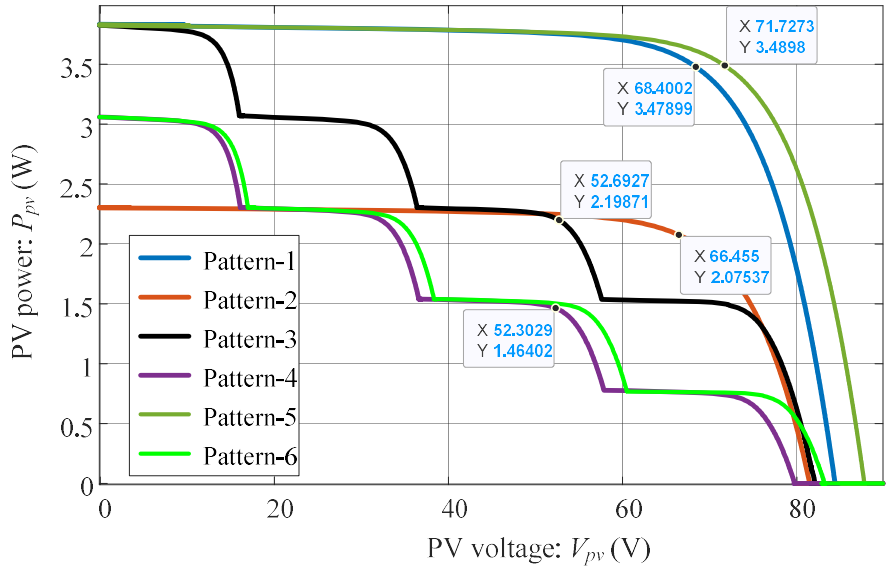

Figure 7. *I-V* graph for different shading patterns

Preprints (www.preprints.org) | NOT PEER-REVIEWED | Posted: 9 February 2022 doi:10.20944/preprints202202.0126.v1

Table 5. Global peak power (G_p) for different patterns

Patterns	G_p (W)	V_{mpp} (V)	I_{mpp} (A)
Pattern-1	237.964	68.4002	3.47899
Pattern-2	137.919	66.455	2.07537
Pattern-3	115.856	52.6927	2.19871
Pattern-4	76.5723	52.3029	1.46402
Pattern-5	250.314	71.7273	3.4898
Pattern-6	80.4385	54.8416	1.46674

From **Figures 6** and **7**, it is seen that under uniform shading conditions (i.e., patterns-1, 2, and 5), the *P-V* and *I-V* graphs produce only one maximum point. However, when partial shading (i.e., patterns-3, 4 and 6) occurs in the PVS, the *P-V* and *I-V* characteristic graphs start producing multiple maximum points due to the working of the bypass diodes in the system. **F**rom the graphs (i.e., patterns-1 to 6), it can be seen that the MPP shifts to the lower left region with the decrease in irradiation and, a decrease in temperature helps to shift the MPP upwards (in **Figure 6**). Meanwhile, the corresponding PV voltage (V_{mpp}) at MPPT will be higher with a high value of peak power under different shading patterns, as observed in **Figure 6**. A similar analysis can be examined in **Figure 7** that the corresponding PV current (I_{mpp}) at MPPT will be higher with a high value of peak power.

3.2. Performance assesemnt of the RIO and PSO algoritms for different benchmark fuctions

A comparative performance assessment of the RIO and PSO is given in **Table 6** for different benchmark functions. In this case study, a minimization problem (i.e., objective function) is considered to get the comparative statistical search performance results of the benchmark functions for 120 numbers of iteration. From **Table 6**, it can be noticed that the data obtained by the RIO algorithm are better than PSO in terms of mean, standard deviation (SD), and best value (f_{min}). Additionally, the convergence characteristic curve for two benchmark functions: Bohachevsky-1 and Langerman-5 is demonstrated in **Figure 8**. **Figure 8** represents that RIO algorithm obtains its global minimal solution for less number of iterations in comparison to PSO. This accomplishment of the RIO algorithm was proved by evaluating the results with that of the PSO for different test functions in [38].

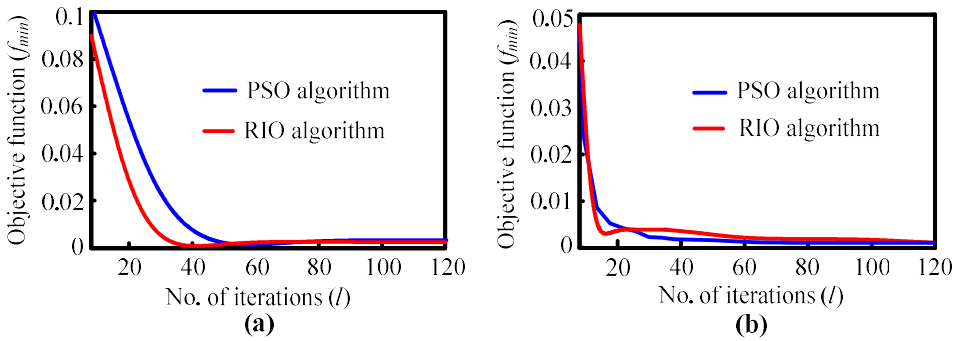

Figure 8. Convergence characteristic graph for: **(a).** Langerman-5 function, **(b).** Bohachevsky-1 function

Preprints (www.preprints.org) | NOT PEER-REVIEWED | Posted: 9 February 2022 doi:10.20944/preprints202202.0126.v1

Table 6. Comparative performance indexes of different test functions

Functions [31]	*DD*	Search space	Statistical values	PSO	RIO*
GoldStein-Price	5	[-200, 200]	Best (f_{min})	8.39e-05	6.56e-05
			Mean	8.40e-05	6.61e-05
			SD	9.20e-07	8.95e-07
Perm	5	[-200, 200]	Best (f_{min})	6.63e-06	5.93e-06
			Mean	6.63e-06	5.99e-06
			SD	0.33e-07	0.31e-07
Langerman-5	5	[-200, 200]	Best (f_{min})	4.86e-07	2.74e-07
			Mean	4.88e-07	2.79e-07
			SD	0.57e-09	0.52e-09
Bohachevsky-1	5	[-200, 200]	Best (f_{min})	8.75e-06	7.41e-06
			Mean	8.77e-06	7.41e-06
			SD	1.83e-08	1.67e-08
Ackley	5	[-200, 200]	Best (f_{min})	0.00e+0	0.00e+0
			Mean	0.00e+0	0.00e+0
			SD	0.00e+0	0.00e+0

**DD* - Number of design variables or dimension, SD- Standard deviation

3.3. Comparison between *PSO and RIO algorithm for MPPT*

To ensure satisfactory performance under partial shading, the RIO-based MPPT recognizes the GMPP. For GMPP tracking, the V_{pv} and the I_{pv} are significant for identifying the MPP. The harvested actual PV power (P_{pv}) of the PVS based on the results obtained from both PSO and proposed RIO algorithms are presented in **Figures 9** and **10**. The simulation results are carried out under the same patterns as shown in *Case-3.1*.

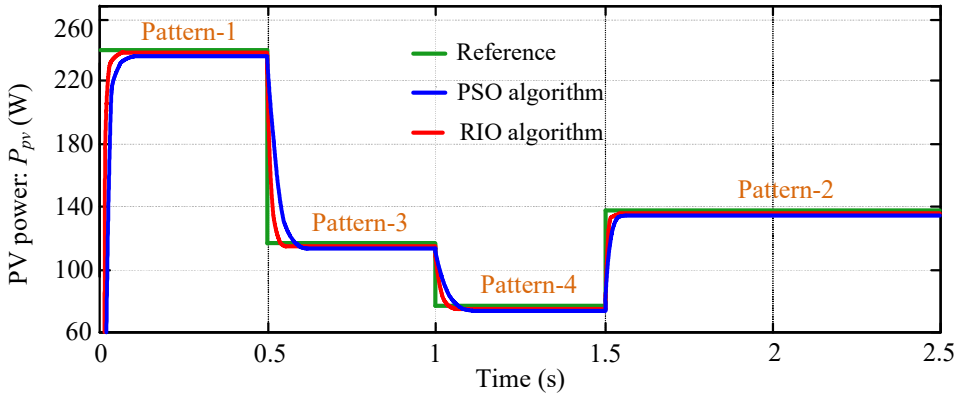

Figure 9. PV system output power performance graph

Preprints (www.preprints.org) | NOT PEER-REVIEWED | Posted: 9 February 2022 doi:10.20944/preprints202202.0126.v1

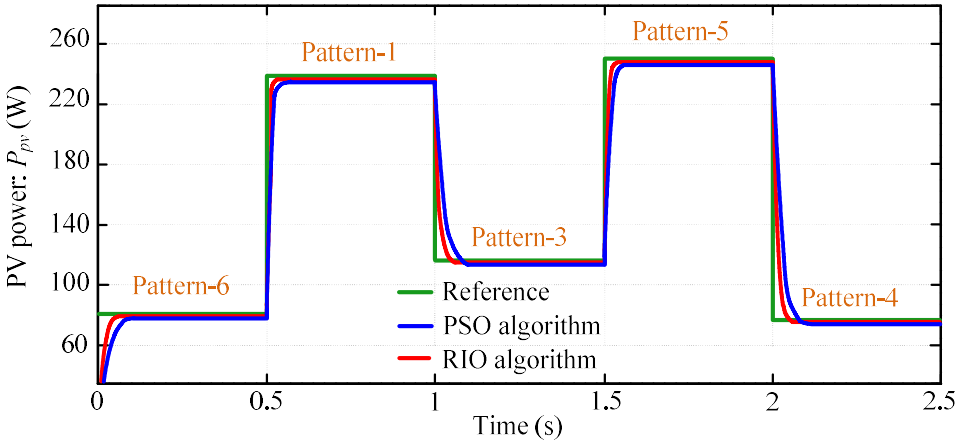

Figure 10. PV system output power performance graph

As shown in **Figures 9-10**, the RIO-based technique tracked the MPP with higher accuracy and extract more power than the PSO from the PV system. The same can be examined in other shading patterns for different values of solar irradiation and temperature. The exact value of the actual power (P_{pv}) tracked by the RIO and PSO of the PVS is presented in **Table 7**, as assessed in **Figures 9** and **10**. Additionally, in order to evaluate the actual MPPT performance attained by both algorithms, the mathematical formulation for MPPT efficiency (η_{MPPT}) is represented as follows [7]:

$$\%\,\eta_{MPPT} = \frac{P_{pv}}{P_{MPPT}} \times 100 \tag{7}$$

where, P_{MPPT} or G_p is the maximum achievable power or true MPP of the PV system (maximum power points are shown in **Figure 6**). P_{pv} is the actual power extracted from the PV array which depends upon the ability of the MPPT to be as close as possible to the true MPP system (**Figures 9** and **10**).

Table 7. Comparative MPPT performance of RIO and PSO

Pattern	Algorithm					
	PSO			RIO*		
	P_{pv} (W)	η_{MPPT} (%)	t_c (ms)	P_{pv} (W)	η_{MPPT} (%)	t_c (ms)
Pattern-1	234.597	98.585	113.964	236.036	99.190	58.451
Pattern-2	135.903	98.538	113.819	136.779	99.174	58.459
Pattern-3	113.651	98.097	124.856	114.502	98.832	67.208
Pattern-4	75.128	98.113	124.572	75.703	98.865	67.211
Pattern-5	246.769	98.584	113.963	248.288	99.191	58.453
Pattern-6	78.922	98.115	124.857	79.526	98.866	67.203

It is true that the higher the MPPT algorithm's accuracy, the higher the η_{MPPT}. The tracking efficiency of the MPPT algorithms for the PV system is shown in **Table 7.** From the above results, it can be concluded that the proposed RIO technique has a good tracking

 doi:10.20944/preprints202202.0126.v1

competency as compared to the PSO-based MPPT technique. Moreover, it can be observed that η_{MPPT} varies with change in partial shading pattern due to the search behavior of the optimization algorithms being random in nature to track the optimal point/solution. Additionally, the convergence speed (i.e., searching process time) is the time that the PV system takes to achieve the steady-state value of P_{pv}. The searching process time (t_c) of the PSO algorithm (**Table 7**) is more than that of the RIO technique for MPPT, as studied in **Figures 9** and **10**. Furthermore, it can be seen that the value of t_c is higher for the partial shading scenario as compared to the symmetrical irradiation on the PV panel.

5. Conclusions and Future Work

In this work, an MPPT technique based on a bio-inspired Roach infestation algorithm is projected to harvest the maximum power from a solar PV under uniform irradiation and PSC uses a step-change in irradiation. The obtained results are examined and evaluated with the PSO algorithm. The results demonstrate that the RIO MPPT contributes better to global maximum power tracking with high accuracy as compared to PSO-based MPPT. In addition, the RIO algorithm is investigated for various benchmark functions and the findings show that RIO is superior to PSO in requirements of computational convergence and optimal solution.

Future research work may be about to investigate the proposed modified RIO algorithm to enhance its search performance for solving different optimization problems. Also, the supremacy of the suggested RIO algorithm can be validated in an experimental hardware platform.

Author Contributions: Conceptualization, C. P.; Methodology, C.P. and N.K.N.; Software, C.P. and N.K.N.; Validation, C.P. and N.K.N.; Formal analysis, C.P. and R.K.C; Writing—original draft preparation, C.P. and N.K.N.; Supervision, C.P.; Writing—review and editing, C.P., and R.K.C. All authors have read and agreed to the published version of the manuscript.

Funding: This research was funded by ARCTIC CENTRE FOR SUSTAINABLE ENERGY (ARC), The University of Tromsø-UiT The Arctic University of Norway, Norway, grant number: ARC-381300.

Institutional Review Board Statement: Not applicable.

Informed Consent Statement: Not applicable.

Data Availability Statement: Not applicable.

Acknowledgments: The authors are very grateful to the Arctic Centre for Sustainable Energy (ARC) and the UiT The Arctic University of Norway, Norway for providing an environment to do this research. Also, the authors acknowledge Prof. Pawan Sharma for the technical help and financial support of the manuscript.

Conflicts of Interest: The authors declare no conflict of interest.

Abbreviations: The following abbreviations are used in this manuscript:

 doi:10.20944/preprints202202.0126.v1

DC	Direct Current
GMPP	Global Maximum Power Point
MATLAB	MATrix LABoratory
MOSFET	Metal-Oxide Field Effect Transistors
MPP	Maximum Power Point
MPPT	Maximum Power Point Tracking
PSC	Partial Shading Condition
PSO	Particle Swarm Optimization
PV	Photovoltaic
PVS	Photovoltaic System
RIO	Roach Infestation Optimization

References

1. Jaganmohan, M., Global cumulative installed solar PV capacity 2000-2019. 2021. https://www.statista.com/statistics/280220/global-cumulative-installed-solar-pv-capacity/.
2. Amin, N., *et al*., *Solar Photovoltaic Technologies: From Inception Toward the Most Reliable Energy Resource*. in Encycl. of Sustainable Technologies, M. A. Abraham Ed. Oxford: Elsevier, 2017, pp. 11-26.
3. Choudhary, P. and Srivastava, R.K., *Sustainability perspectives- a review for solar photovoltaic trends and growth opportunities*. Journal of Cleaner Production, 2019, **227**, pp. 589-612.
4. Mao, M., *et al*., *Classification and summarization of solar photovoltaic MPPT techniques: A review based on traditional and intelligent control strategies*. Energy Reports, *2020*, **6**, pp. 1312-1327.
5. Obeidat, F., *A comprehensive review of future photovoltaic systems*. Solar Energy, 2018, **163**, pp. 545-551.
6. Lupangu, C., and Bansal, R.C., *A review of technical issues on the development of solar photovoltaic systems*. Renewable and Sustainable Energy Reviews, 2017, **73**, pp. 950-965.
7. Pradhan; C., *et al*., *Coordinated Power Management and Control of Standalone PV-Hybrid System With Modified IWO-Based MPPT*. IEEE Systems Journal, 2021, **15**(3), pp. 97-108.
8. Javed, M.Y., *et al*., *A Comprehensive Review on a PV Based System to Harvest Maximum Power*. Electronics, 2019, 11(3), pp. 1-66.
9. Raghavendra, K.V., *et al*., *A Comprehensive Review of DC–DC Converter Topologies and Modulation Strategies with Recent Advances in Solar Photovoltaic Systems*. Electronics, 2020, 9(1), pp. 1-41.
10. Li, X., *et al*., *Comprehensive Studies on Operational Principles for Maximum Power Point Tracking in Photovoltaic Systems*. IEEE Access, 2019. 7, pp. 121407-121420.
11. Li, G., *et al*., *Application of Bio-inspired Algorithms in Maximum Power Point Tracking for PV Systems under Partial Shading Sonditions – A review*. Renewable and Sustainable Energy Reviews, 2018, **81**, pp. 840-873.
12. Paulo, A.F.de, and Porto, G.S., *Evolution of collaborative networks of solar energy applied technologies*. Journal of Cleaner Production, 2018, **204**, pp. 310-320.
13. Kermadi, M., and Berkouk, E.M., *Artificial intelligence-based maximum power point tracking controllers for Photovoltaic systems: Comparative study*. Renewable and Sustainable Energy Reviews, **2017**, 69, pp. 369-386.
14. Da Luz, C.M.A., Vicente, E.M., and Tofoli, F.L., *Experimental evaluation of global maximum power point techniques under partial shading conditions*. Solar Energy, 2020. 196, pp. 49-73.
15. Ko, J.S., Huh, J.H.,and Kim, J.C., *Overview of Maximum Power Point Tracking Methods for PV System in Micro Grid*. Electronics, 2020, 9(5), pp. 1-22.
16. Motahhir, S., *et al*, *The most used MPPT algorithms: review and the suitable low-cost embedded board for eachalgorithm*. *Journal of Cleaner Production*, 2020; **246**, no. 1, pp. 1-17.
17. Owusu-Nyarko, I., *et al*, *Modified Variable Step-Size Incremental Conductance MPPT Technique for Photovoltaic Systems*. Electronics, 2021, **10**(19), pp. 1-18.
18. Ahmed, J., and Salam, Z., *A Modified P&O Maximum Power Point Tracking Method with Reduced Steady State Oscillation and Improved Tracking Efficiency*. *IEEE Transactions on Sustainable Energy*; 2016, **7**(4), pp. 1506-1515.
19. Rawat, R., and Chandel, S., *Hill Climbing Techniques for Tracking Maximum Power Point in Solar Photovoltaic Systems - A Review*. Special Issue of International Journal of Sustainable Development and Green Economics, 2013, 2, pp. 90-95.
20. Subramanian, V., *et al*., *Modeling and Analysis of PV System with Fuzzy Logic MPPT Technique for a DC Microgrid under Variable Atmospheric Conditions*. Electronics, 2021, **10**(20), pp. 5-16.

21. Kulaksiz, A.A., and Akkaya, R., *A Genetic Algorithm Optimized ANN based MPPT Algorithm for a Stand-alone PV System with Induction Motor Drive*. Solar Energy; 2012, **86**(9), pp. 2366-2375.
22. Huang, Y.P., Huang, M.Y., and Ye, C.E., *A Fusion Firefly Algorithm with Simplified Propagation for Photovoltaic MPPT under Partial Shading Conditions*. IEEE Transactions on Sustainable Energy, 2020, **11**(4), pp. 2641-2652.
23. Ishaque, K., and Salam, Z., *A Deterministic Particle Swarm Optimization Maximum Power Point Tracker for Photovoltaic System under Partialshading Condition*. IEEE Transactions on Industrial Electronics, 2013, **60**(8), pp. 3195-3207.
24. Titri, S., *et al*., *A New MPPT Controller Based on the Ant Colony Optimization Algorithm for Photovoltaic Systems under Partial Shading Conditions*. Applied Soft Computing, 2017, **58**, pp. 465-479.
25. Zaki Diab, A.A., and Rezk, H., *Global MPPT Based on Flower Pollination and Differential Evolution Algorithms to Mitigate Partial Shading in Building Integrated PV System*. Solar Energy, 2017, **157**, pp. 171-186.
26. Senapati, M. K., Pradhan, C., and Calay, R.K., *A computational intelligence based maximum power point tracking for photovoltaic power generation system with small-signal analysis*. Optimal Control Applications and Methods, 2021, **32**(2), pp. 1–20.
27. Mirza, A. Feroz, *et al*., *A Salp Swarm Optimization based MPPT Technique for Harvesting Maximum Energy from PV Systems under Partial Shading Conditions*. Energy Conversion and Management, 2020, **209**, pp. 11625.
28. Liao, C.Y., *et al*., *An Improved Bat Algorithm for More Efficient and Faster Maximum Power Point Tracking for a Photovoltaic System Under Partial Shading Conditions*. IEEE Access, 2020. 8, pp. 96378-96390.
29. Rehman, H., *et al*., *Neighboring-Pixel-Based Maximum Power Point Tracking Algorithm for Partially Shaded Photovoltaic (PV) Systems*. Electronics, 2022, 11(3), pp. 1-13.
30. González-Castaño., C., et al., *An MPPT Strategy Based on a Surface-Based Polynomial Fitting for Solar Photovoltaic Systems Using Real-Time Hardware*. Electronics, 2021, 10(2), pp. 1-22.
31. Pervez, I., *et al*., *Rapid and Robust Adaptive Jaya (Ajaya) based Maximum Power Point Tracking of a PV-based Generation System*. IEEE Access, 2020. **9**, pp. 48679-48703.
32. Pervez, I., *et al*., Most Valuable Player Algorithm Based Maximum Power Point Tracking for a Partially Shaded PV Generation System. IEEE Transactions on Sustainable Energy, 2021, **12**(4), pp. 1876-1890.
33. Pradhan, C., and Bhende, C.N., *Online Load Frequency Control in Power Systems using Modified Jaya Optimization Algorithm*. Engineering Applications of Artificial Intelligence, 2019, **77**, pp. 212-228.
34. Pradhan, C., and Gjengedal, T., *Adaptive Jaya Algorithm for Optimized PI-PD Cascade Controller of Load Frequency Control in Inter-connected Two-Area Power System*. International Conference on Smart Systems and Technologies (SST), 2020, pp. 181-186.
35. Ali, A., *et al*, *Investigation of MPPT Techniques Under Uniform and Non-Uniform Solar Irradiation Condition–A Retrospection*. IEEE Access, 2020, **8**, pp. 127368-127392.
36. Dileep, G., and Singh, S.N., *Selection of non-isolated DC-DC converters for solar photovoltaic system*. Renewable and Sustainable Energy Reviews, 2017, **76**, pp. 1230-1247.
37. Asadi, F., and Eguchi, K., Dynamics and Control of DC-DC Converters: Synthesis Lectures on Power Electronics, 2018, **6**(1), pp. 1-241.
38. Havens, T.C., *et al.*, Roach Infestation Optimization," in *2008 IEEE Swarm Intelligence Symposium*, 21-23 Sept. 2008, pp. 1-7.
39. Pradhan, C., and Gjengedal, T., *A Novel Fuzzy Adaptive Jaya Optimization for Automatic Generation Control in Multi-Area Power System*. IEEE 17th India Council International Conference (INDICON), 2020, pp. 1-6.